Inhomogeneous pairing in highly disordered *s*-wave superconductors

Amit Ghosal, Mohit Randeria, and Nandini Trivedi
Department of Theoretical Physics, Tata Institute of Fundamental Research, Homi Bhabha Road, Colaba, Mumbai 400005, India
(Received 13 March 2001; published 29 November 2001)

We study a simple model of a two-dimensional *s*-wave superconductor in the presence of a random potential as a function of disorder strength. We first use the Bogoliubov–de Gennes (BdG) approach to show that, with increasing disorder, the pairing amplitude becomes spatially inhomogeneous, and the system cannot be described within conventional approaches for studying disordered superconductors that assume a uniform order parameter. In the high-disorder regime, we find that the system breaks up into superconducting islands, with large pairing amplitude, separated by an insulating sea. We show that this inhomogeneity has important implications for the physical properties of this system, such as superfluid density and the density of states. We find that a finite spectral gap persists in the density of states, even in the weak-coupling regime, for all values of disorder, and we provide a detailed understanding of this remarkable result. We next generalize Anderson's idea of the pairing of exact eigenstates to include an inhomogeneous pairing amplitude, and show that it is able to qualitatively capture many of the nontrivial features of the full BdG analysis. Finally, we study the transition to a gapped insulating state driven by quantum phase fluctuations about the inhomogeneous superconducting state.

DOI: 10.1103/PhysRevB.65.014501 PACS number(s): 74.20.Mn, 74.20.−z, 71.55.Jv

I. INTRODUCTION

Studies of the interplay between localization and superconductivity in low dimensions have got a boost from experiments on superconducting films,[1,2] which show a dramatic reduction in T_c with increasing disorder and eventually a transition to an insulating state above a critical disorder strength beyond which resistivity increases with decreasing T. The data in the vicinity of the transition often seem to exhibit scaling behavior, suggesting a continuous, disorder-driven superconductor (SC) to insulator (I) quantum phase transition at $T=0$.

The physics of these highly disordered films is outside the domain of validity of the early theories of dirty superconductors, due to Anderson[3] and to Abrikosov and Gorkov,[4] which are applicable only in the low-disorder regime where the mean free path is much longer than the inverse Fermi wave vector. The effect of strong disorder on superconductivity is a challenging theoretical problem, as it necessarily involves both interactions and disorder.[5]

Several different theoretical approaches have been taken in the past. First, there are various mean-field approaches that either extend Anderson's pairing of time-reversed exact eigenstates or extend the diagrammatic method to high disorder regimes; see, e.g., Refs. 5–13. In much of the present work we will also make use of mean-field theories, which, however, differ from all previous works in a crucial aspect: we will *not* make any assumption about the spatial uniformity of the local pairing amplitude Δ. Using the Bogoliubov–de Gennes (BdG) approach, as well as a simpler variational treatment using exact eigenstates, we will show that outside of the weak-disorder regime, the spatial inhomogeneity of Δ becomes very important, and leads to new and unanticipated observable effects, most importantly a nonvanishing spectral gap at large disorder.[14]

The other point of view, primarily due to Fisher and collaborators,[15] has been to focus on the universal critical properties in the vicinity of the superconductor-insulator transition (SIT). These authors have argued that fermionic degrees of freedom should be unimportant at the transition, and the transition should be in the same universality class as the dirty boson problem. As we shall see, our results on a simple fermionic model explicitly demonstrate how the electrons remain gapped through the transition, which is then indeed in a bosonic universality class. The SIT will be shown to be driven by quantum phase fluctuations about the inhomogeneous mean field state.[16]

We now summarize our main results for a two-dimensional (2D) disordered *s*-wave SC described by the model of Sec. II.

(1) With increasing disorder, the distribution $P(\Delta)$ of the local pairing amplitude $\Delta(\mathbf{r}) \propto \langle c_\downarrow(\mathbf{r}) c_\uparrow(\mathbf{r}) \rangle$ obtained within an inhomogeneous BdG framework becomes very broad, eventually developing considerable weight near $\Delta \approx 0$. In contrast, conventional mean-field approaches assume a spatially uniform Δ.

(2) The spectral gap in the one-particle density of states (DOS) persists even at high disorder in spite of a growing number of sites with $\Delta(\mathbf{r}) \approx 0$. A detailed understanding of this surprising effect emerges from a study of the spatial variation of $\Delta(\mathbf{r})$, which shows the formation of locally superconducting ''islands'' separated by a nonsuperconducting sea and a very special correlation between $\Delta(\mathbf{r})$ and the BdG eigenfunctions.

(3) Even though our model is (''homogeneously'') disordered on a microscopic scale, the combination of the pairing interaction and strong disorder leads to the formation of inhomogeneous structures reminiscent of granular systems: SC islands separated by an insulating sea.

(4) We have a clear prediction for scanning tunneling microscopy (STM) measurements that should show a small SC gap with a pile-up in the local DOS when the tip is on a SC island and a larger pseudogaplike feature in non-SC regions.

(5) Not only does the spectral gap in the total DOS persist

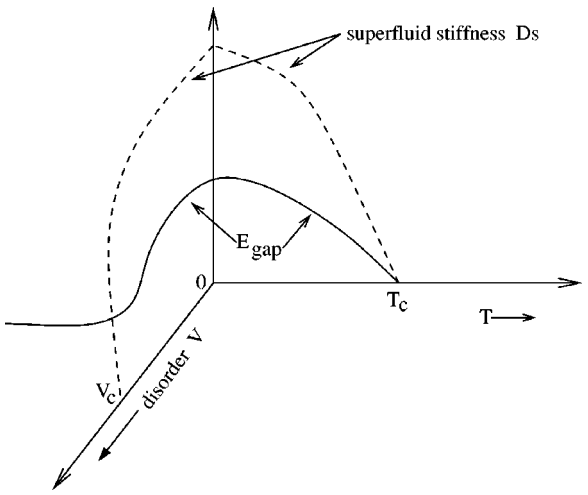

FIG. 1. Schematic behavior of superfluid stiffness D_s and energy gap $E_{\rm gap}$ as a function of temperature T and disorder V for the model in Eq. (1). For $V=0$, both D_s and $E_{\rm gap}$ vanish at the critical temperature T_c as expected for a weak-coupling SC. However, for $T=0$ the behavior is very unusual with D_s vanishing at a critical V_c but $E_{\rm gap}$ remaining finite (and even increasing with disorder) at large V.

in the disordered insulator, but it *increases* with increasing disorder. We have generalized the ''pairing of exact eigenstates'' formalism to allow for an inhomogeneous pairing amplitude, and find that this unusual behavior of the gap is explained in terms of the localization properties of the single-particle wave functions.

(6) There is substantial reduction in the superfluid stiffness and off-diagonal correlations with increasing disorder. However, the spatial amplitude fluctuations, in response to the random potential, cannot by themselves destroy superconductivity.

(7) We include the effects of phase fluctuations about the inhomogeneous SC state, using a quantum XY model whose parameters, compressibility, and phase stiffness, are obtained from the BdG mean-field results. A simple analysis of this effective model within a self-consistent harmonic approximation leads to a transition from the superconductor to a gapped insulator.

Our results on the disorder dependence of the spectral gap and superfluid stiffness are shown schematically in Fig. 1. While the superfluid density D_s decreases with increasing disorder ultimately vanishing at a critical disorder strength, the energy gap always remains finite, and shows an unusual nonmonotonic behavior: it initially decreases with disorder but remains finite and even increases for large disorder. Note the difference between the finite temperature transition in the nondisordered case and the disorder-driven $T=0$ transition. The $V=0$ transition at T_c is driven at weak coupling by the collapse of the gap. In contrast the $T=0$ transition at V_c is driven by a vanishing superfluid stiffness even though the gap remains finite.

Some of the results described here were first reported in a Letter.[14] The results reported here are at much weaker coupling, which is the case of experimental interest in disordered SC films. The earlier work was limited to intermediate coupling, in part, for numerical ease (smaller system sizes are sufficient for shorter coherence lengths) and, in part, to make comparisons with quantum Monte Carlo (QMC) studies[17] of the same model. The extension to the weak-coupling region, where the zero-disorder energy gap is much smaller than the superfluid stiffness, has been made possible by technical improvements in solving the BdG equations self-consistently on larger lattices, and by the semianalytical treatment of the pairing of exact eigenstates.

The rest of this paper is organized as follows: In Sec. II we describe our model for the disordered SC. In Sec. III we briefly describe the inhomogeneous BdG mean-field method, and discuss in detail the results of this analysis. We focus on the disorder dependence of various physically interesting quantities, such as pairing amplitude, density of states, energy gap, order parameter, and the superfluid density. In Sec. IV we develop the pairing of exact eigenstates theory, taking into account the inhomogeneity of the pairing amplitude. Phase fluctuations are discussed in Sec. V and the phase diagram based on our calculations is described in Sec. VI. In Sec. VII we discuss some implications for experiments, including a prediction for STM measurements and some comments on ''homogeneously'' disordered versus granular SC films.

II. MODEL

We describe a 2D s-wave SC in the presence of *nonmagnetic* impurities by the Hamiltonian $\mathcal{H}=\mathcal{H}_0+\mathcal{H}_{\rm int}$,

$$\mathcal{H}_0=-t\sum_{\langle ij\rangle,\sigma}(c^\dagger_{i\sigma}c_{j\sigma}+\text{H.c.})+\sum_{i,\sigma}(V_i-\mu)n_{i\sigma}$$

$$\mathcal{H}_{\rm int}=-|U|\sum_i n_{i\uparrow}n_{i\downarrow}. \qquad (1)$$

Here $c^\dagger_{i\sigma}$ ($c_{i\sigma}$) is the electron creation (destruction) operator with spin σ on a site $\mathbf{r}_i$ of a square lattice with lattice spacing $a=1$, t is the near-neighbor hopping, $|U|$ is the pairing interaction, $n_{i\sigma}=c^\dagger_{i\sigma}c_{i\sigma}$, and μ is the chemical potential. The impurity potential is defined by an independent random variable V_i uniformly distributed over $[-V,V]$, at each site $\mathbf{r}_i$. V thus controls the strength of the disorder.

Before proceeding, we comment on the choice of the Hamiltonian, Eq. (1). The effects of Coulomb repulsion are neglected here in a spirit similar to the Anderson localization problem.[18] Despite this simplification, Anderson localization has had a profound impact on disordered electron systems, and a complete understanding of interactions in the presence of disorder is still an open problem. Similarly the Hamiltonian we study is a minimal model containing the interplay of superconductivity and localization: for zero disorder $V=0$ it describes s-wave superconductivity and for $|U|=0$ it reduces to the (noninteracting) Anderson localization problem. We feel that it is very important to first understand the physics of this simple model before putting in the additional complication of Coulomb effects.[19]

We next comment on the choice of parameters. We have studied the model (1) for a range of parameters, $0.8 \leqslant |U|/t \leqslant 8$, $0.2 \leqslant \langle n \rangle \leqslant 0.875$, and a wide range of disorder on lattices of sizes up to $N = 36 \times 36$. In Ref. 14 we reported results mainly for $|U|/t = 4$. Here we focus on weaker coupling $|U|/t = 1.5$ and $\langle n \rangle = 0.875$ on systems of typical size 24×24. We have taken care to work on systems with linear size larger than the coherence length ξ.[20]

III. BOGOLIUBOV–DE GENNES MEAN-FIELD THEORY

We begin with a very brief review of the BdG mean-field theory,[21] mainly to introduce notation. The mean-field decomposition of the interaction term gives expectation values to the local pairing amplitude and local density,

$$\Delta(\mathbf{r}_i) = -|U|\langle c_{i\downarrow} c_{i\uparrow}\rangle, \quad \langle n_{i\sigma}\rangle = \langle c^\dagger_{i\sigma} c_{i\sigma}\rangle, \tag{2}$$

and yields an effective quadratic Hamiltonian

$$\mathcal{H}_{\rm eff} = -t \sum_{\langle ij\rangle,\sigma} (c^\dagger_{i\sigma} c_{j\sigma} + \text{H.c.}) + \sum_i (V_i - \tilde{\mu}_i) n_{i\sigma} + \sum_i [\Delta(\mathbf{r}_i) c^\dagger_{i\uparrow} c^\dagger_{i\downarrow} + \Delta^*(\mathbf{r}_i) c_{i\uparrow} c_{i\downarrow}], \tag{3}$$

where $\tilde{\mu}_i = \mu + |U|\langle n_i\rangle/2$ incorporates the site-dependent Hartree shift. Here $\langle n_i\rangle = \Sigma_\sigma \langle n_{i,\sigma}\rangle$. $\mathcal{H}_{\rm eff}$ is diagonalized by the transformation

$$c_{i\uparrow} = \sum_n [\gamma_{n\uparrow} u_n(\mathbf{r}_i) - \gamma^\dagger_{n\downarrow} v^*_n(\mathbf{r}_i)],$$

$$c_{i\downarrow} = \sum_n [\gamma_{n\downarrow} u_n(\mathbf{r}_i) + \gamma^\dagger_{n\uparrow} v^*_n(\mathbf{r}_i)], \tag{4}$$

where γ and $\gamma^\dagger$ are the quasiparticle operators. $u_n(\mathbf{r}_i)$ and $v_n(\mathbf{r}_i)$, which satisfy $\Sigma_n |u_n(\mathbf{r}_i)|^2 + |v_n(\mathbf{r}_i)|^2 = 1$ for each $\mathbf{r}_i$, are obtained from

$$\begin{pmatrix} \hat{K} & \hat{\Delta} \\ \hat{\Delta}^* & -\hat{K}^* \end{pmatrix} \begin{pmatrix} u_n(\mathbf{r}_i) \\ v_n(\mathbf{r}_i) \end{pmatrix} = E_n \begin{pmatrix} u_n(\mathbf{r}_i) \\ v_n(\mathbf{r}_i) \end{pmatrix}, \tag{5}$$

where the excitation eigenvalues $E_n \geqslant 0$. $\hat{K} u_n(\mathbf{r}_i) = -t \Sigma_{\hat{\boldsymbol{\delta}}} u_n(\mathbf{r}_i + \hat{\delta}) + (V_i - \tilde{\mu}_i) u_n(\mathbf{r}_i)$, where $\hat{\boldsymbol{\delta}} = \pm\hat{\mathbf{x}}, \pm\hat{\mathbf{y}}$, and $\hat{\Delta} u_n(\mathbf{r}_i) = \Delta(\mathbf{r}_i) u_n(\mathbf{r}_i)$, and similarly for $v_n(\mathbf{r}_i)$. The self-consistency conditions are given by

$$\Delta(\mathbf{r}_i) = |U| \sum_n u_n(\mathbf{r}_i) v^*_n(\mathbf{r}_i),$$

$$\langle n_i\rangle = 2 \sum_n |v_n(\mathbf{r}_i)|^2. \tag{6}$$

We solve the BdG equations (5) on a finite lattice of N sites with periodic boundary conditions, as follows. Starting with an initial guess for the pairing amplitude $\{\Delta(\mathbf{r}_i)\}$ and the chemical potential $\{\tilde{\mu}_i\}$ at each site, we numerically determine the eigenvalues E_n and eigenvectors $(u_n(\mathbf{r}_i), v_n(\mathbf{r}_i))$ of Eq. (5). We then compute $\{\Delta(\mathbf{r}_i)\}$ and $\{\langle n_i\rangle\}$ from Eq. (6). If these values differ from the initial ones, the whole process is iterated with a new choice of $\{\Delta(\mathbf{r}_i)\}$ and $\{\langle n_i\rangle\}$ in Eq. (5) until *self-consistency is achieved at each site*. The chemical potential μ is determined by $(1/N)\Sigma_i n_i = \langle n\rangle$, the given average density. Note that $\Delta(\mathbf{r}_i)$, $u(\mathbf{r}_i)$, and $v(\mathbf{r}_i)$ can be chosen to be real in the absence of a magnetic field.

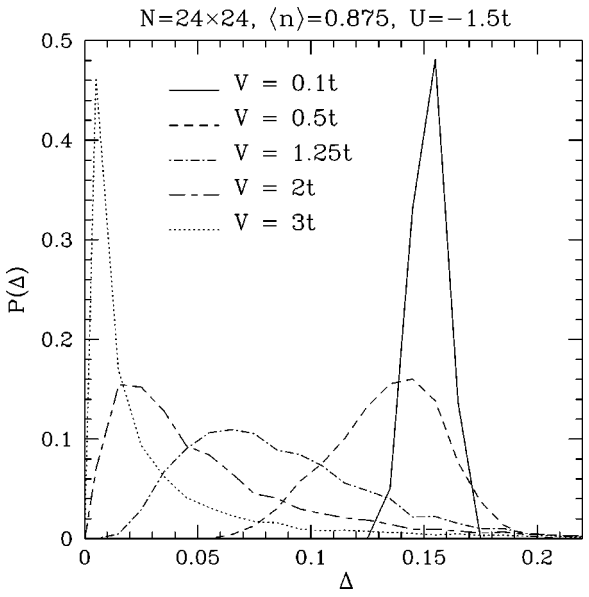

FIG. 2. Distribution of the local pairing amplitude $\Delta(\mathbf{r})$ for various disorder strengths. At low disorder the distribution $P(\Delta)$ is sharply peaked around $\Delta_0 \approx 0.15$, the pure BCS value for $|U| = 1.5t$. $P(\Delta)$ becomes broad with increasing V and finally at a very large disorder gains significant weight near $\Delta \approx 0$.

We have checked that the same solution is obtained for different initial guesses. However, the number of iterations to obtain self-consistency grows with disorder. All the results are averaged over 12–15 different realizations of disorder for a given disorder strength V.

We emphasize that, while the BdG theory has been extensively used recently for disordered d-wave superconductors,[22,23] in many cases full self-consistency at each site is not attained, and in almost no case, except for Refs. 14 and 23, has the inhomogeneous Hartree shift been retained. The nontrivial results obtained in this paper depend in a crucial way on fully self-consistent inhomogeneous solutions, as will become clear.

A. Local pairing amplitudes and off-diagonal long-range order

The ground state energy of the inhomogeneous BdG solution is always lower than that obtained by forcing a uniform pairing amplitude, with the difference between them increasing with V. In Fig. 2 we plot the distribution $P(\Delta)$ of the self-consistent local pairing amplitude $\Delta(\mathbf{r}_i)$ for several values of the disorder V. For $V = 0$ the BdG solution has a uniform pairing amplitude $\Delta_0 \simeq 0.153t$, the BCS value. For low disorder $V = 0.1t$, the distribution $P(\Delta)$ has a sharp peak about Δ_0, which justifies the use of a homogeneous mean-field theory (MFT) for small disorder (as, e.g., in the deriva-

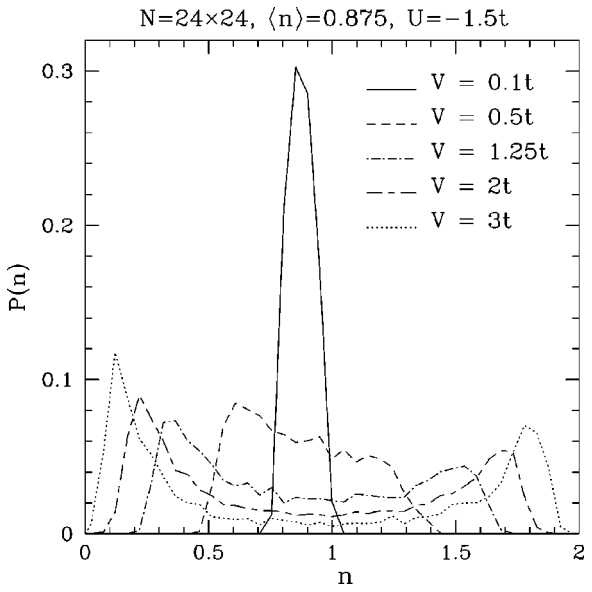

FIG. 3. The distribution of the local density $n(\mathbf{r})$ for various disorder strengths. At low disorder the distribution is sharply peaked around the average density $\langle n\rangle = 0.875$. $P(n)$ becomes broad with increasing V and for large disorder evolves towards a bimodal distribution with empty and doubly occupied sites.

tion of Anderson's theorem). With increasing disorder $V \sim 1t$, the distribution $P(\Delta)$ becomes broad and the assumption of a uniform Δ breaks down. With further increase of disorder $V \sim 2t$, $P(\Delta)$ becomes highly skewed with weight building up near $\Delta \approx 0$.

Similar $P(\Delta)$ were obtained for different values of the attraction $|U|$. We have found that, for the same disorder V, the fluctuations in $\Delta(\mathbf{r}_i)$ are larger for higher values of the attraction $|U|$.

The distribution of the local pairing amplitude $P(\Delta)$ should be contrasted with the distribution of local density $P(n)$, which is also inhomogeneous with increasing disorder but very distinct, as shown in Fig. 3. As a function of disorder it evolves from being sharply peaked about the average $\langle n\rangle$ at low V towards an almost bimodal distribution for large V, with sites being either empty (corresponding to high mountains in the random potential topography) or doubly occupied (in the deep valleys of the random potential). Later, we will also contrast the spatial correlations between the local pairing amplitudes and the local densities.

The off-diagonal long-range order (ODLRO) is defined by the long-distance behavior of the (disorder averaged) correlation function $\langle c^\dagger_{i\uparrow} c^\dagger_{i\downarrow} c_{j\downarrow} c_{j\uparrow}\rangle \to \Delta^2_{\mathrm{OP}}/|U|^2$ for $|\mathbf{r}_i - \mathbf{r}_j| \to \infty$. In the SC state the order parameter Δ_{OP} is finite whereas in the non-SC state the off-diagonal correlations decay to zero at large distances so $\Delta_{\mathrm{OP}} = 0$. It can be shown that $\Delta_{\mathrm{OP}} \simeq \int d\Delta \Delta P(\Delta)$, i.e., it is the average value of the local pairing amplitude. Our calculations show that Δ_{OP}, which is identical to Δ_0 in the limit $V = 0$, is substantially reduced by disorder as seen in Fig. 5.

B. Density of states and energy gap

In Fig. 4 we show the behavior of the single-particle density of states (DOS) given by

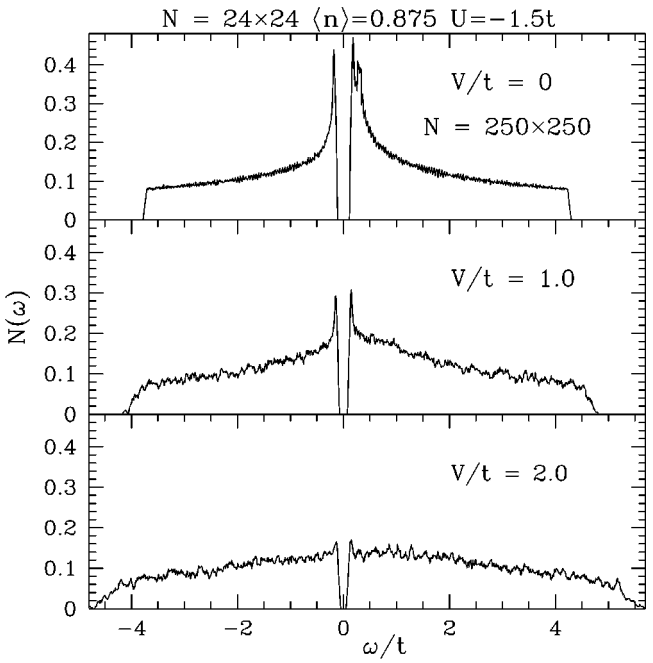

FIG. 4. Density of states $N(\omega)$ for three disorder strengths V. With increasing disorder the singular pile-up at the gap edge smears out pushing states towards higher energies. Surprisingly, the spectral gap remains finite even at large V.

$$N(\omega) = \frac{1}{N} \sum_{n,\mathbf{r}_i} [u_n^2(\mathbf{r}_i)\,\delta(\omega - E_n) + v_n^2(\mathbf{r}_i)\,\delta(\omega + E_n)] \quad (7)$$

averaged over disorder. With increasing disorder the DOS pile-up at the gap edge is progressively smeared out and

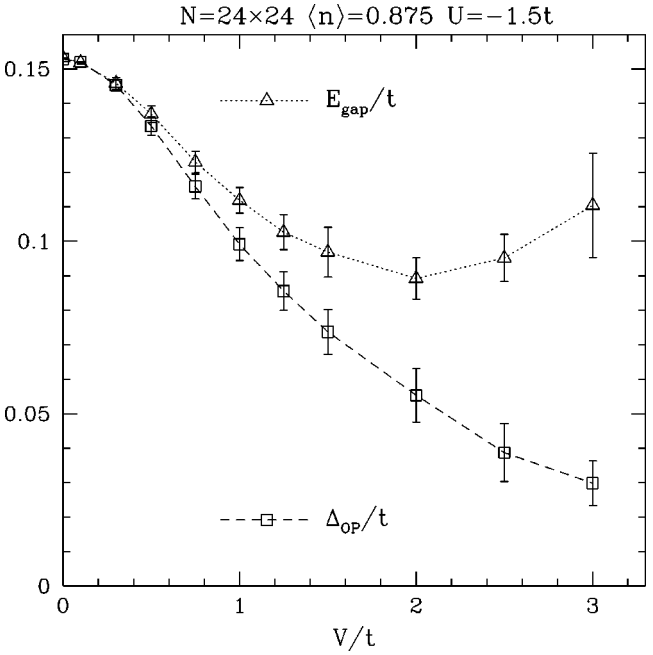

FIG. 5. The spectral gap E_{gap} and order parameter Δ_{OP} as a function of the disorder. For small V they are the same (as expected), but quite different, both in value and functional form, at large disorder.

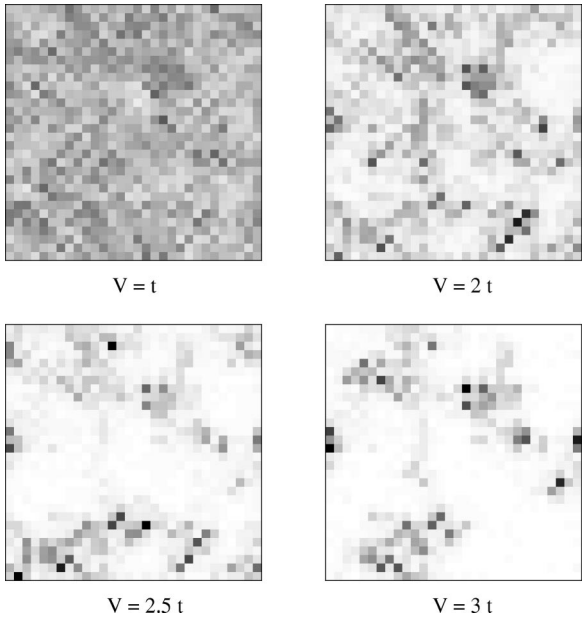

FIG. 6. Gray-scale plot for the spatial variation of the local pairing amplitude $\Delta(\mathbf{r})$ for a particular realization of the random potential (same in all the panels) but with increasing disorder strength. Note that at large V the system generates ''SC islands'' (dark regions) with large pairing amplitude separated by an insulating ''sea'' (white regions) with negligible pairing amplitude.

states are pushed to higher energies. However, the gap in the spectrum remains finite.

The energy gap E_{gap} is obtained directly as the lowest eigenvalue of the BdG matrix in Eq. (5). We plot the evolution of E_{gap} with disorder in Fig. 5, and see that it not only remains finite, it even increases at high disorder.

These results are counterintuitive. Given the broad distribution $P(\Delta)$ (Fig. 2) at high disorder, with $\Delta \approx 0$ at many sites, one might have expected the spectral gap to also collapse. However, this expectation is based on an (incorrect) identification of the average pairing amplitude, or order parameter Δ_{OP}, with the spectral gap E_{gap}. While the two coincide at small disorder strengths, we see from Fig. 5 that the two show qualitatively different behavior at high disorder. It turns out that important insight into these puzzling results can be obtained by looking at the inhomogeneities in $\Delta(\mathbf{r}_i)$ in real space, as discussed below.

C. Formation of superconducting islands

In Fig. 6 we see the evolution of the spatial distribution of the local pairing amplitude for a particular realization of the random potential with increasing disorder strength V. Though the random potential V_i is completely uncorrelated from site to site, the system generates, with increasing disorder, spatially correlated clusters of sites with large $\Delta(\mathbf{r}_i)$, or ''SC islands,'' which are separated from one another by regions with very small $\Delta(\mathbf{r}_i)$. The size of the SC islands is the coherence length, which is controlled by the attraction $|U|$ and the disorder V.

We would like to emphasize that formation of the ''SC islands'' is not simply related to the inhomogeneous electron density profile in the presence of disorder. In Figs. 7(a) and 7(c) we show density $n(\mathbf{r}_i)$ and $\Delta(\mathbf{r}_i)$ in a gray-scale plot for a particular realization of the random potential at a disorder strength $V=3t$. As expected, the density varies rapidly *on the scale of the lattice constant* in response to the random potential. This is emphasized by the density-density correlations being extremely short ranged in Fig. 7(b). In contrast, the pairing amplitude shows structure, i.e., the formation of SC islands on the scale of the coherence length ξ, which is several lattice spacings. (The coherence length[20] of the corresponding nondisordered system is $\xi_0 \simeq 10$).

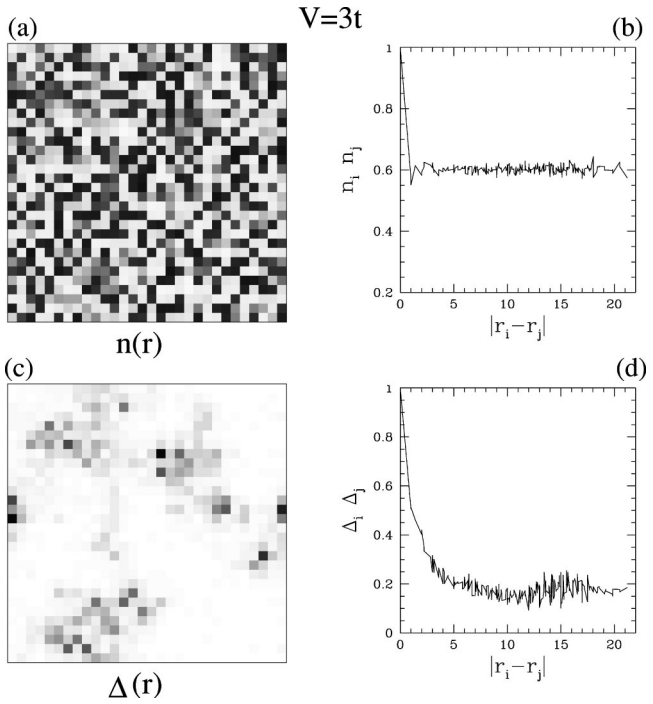

FIG. 7. (a) Gray-scale plot of density n_i for a given disorder realization, for $V=3t$, with darker regions indicating higher densities. (b) Plot of disorder-averaged correlation function $\overline{n_i n_j}$ as a function of the distance $r \equiv |\mathbf{r}_i - \mathbf{r}_j|$. Note that density correlations decay within a lattice constant. The y axis is scaled by $\overline{n_i^2}$ (a V-dependent number, which is 1.27 for $V=3$) so that the function is normalized to unity at $r=0$. (c) Gray-scale plot of of pairing amplitude $\Delta(\mathbf{r}_i)$ on the lattice for the same V and same realization as in (a). (d) The disorder-averaged correlation function $\overline{\Delta(\mathbf{r}_i)\Delta(\mathbf{r}_j)}$ (normalized to be unity at zero separation) showing that the correlations persist to distances of order several lattice spacings, which is the size of the SC islands.

We next ask: where (in space) are these ''SC islands'' formed? This will be very important in our understanding of the origin of the finite energy gap at large disorder. By correlating the locations of the islands with the underlying random potential for many different realizations, we find that large $\Delta(\mathbf{r})$ occurs in regions where $|V_i - \tilde{\mu}_i|$ is small and allows for considerable particle-hole mixing. On the other hand, deep valleys and high mountains in the potential energy landscape contain a fixed number of particles per site: two on a valley site or zero on a mountain site. As a result the local pairing amplitude vanishes in such regions.

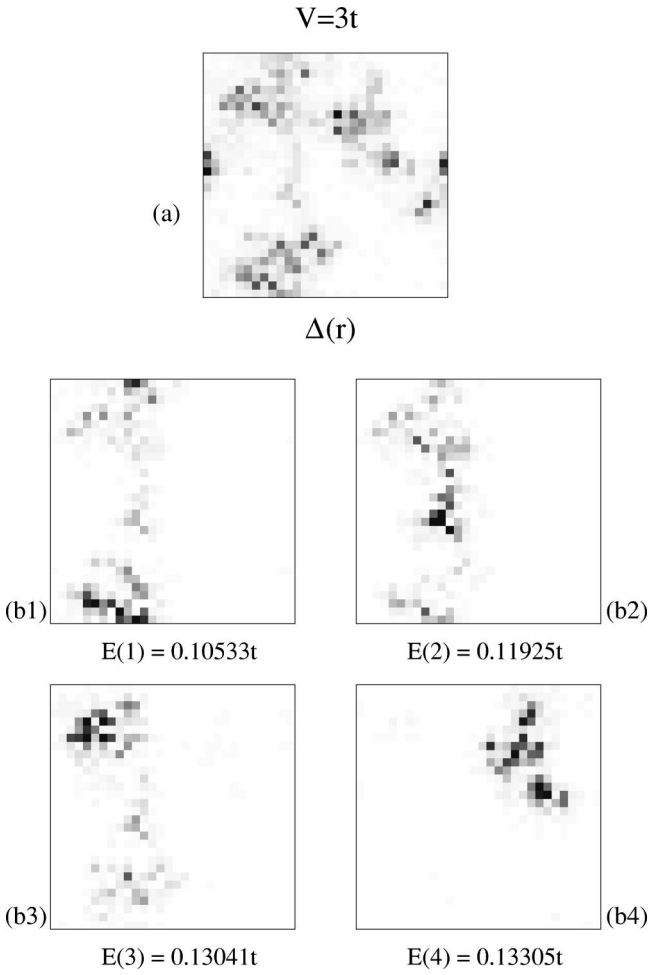

FIG. 8. (a) Gray-scale plot of the local pairing amplitude $\Delta(\mathbf{r}_i)$ for a particular realization of the random potential at $V=3t$. (b1)–(b4) are gray-scale plots of $|u_n(\mathbf{r})|^2+|v_n(\mathbf{r})|^2$ for the lowest four excitations $(n=1,\ldots,4)$ with corresponding eigenvalues $E(1),\ldots,E(4)$. We see that a particle added to (or extracted from) the system has a high probability of being found in regions where $\Delta(\mathbf{r}_i)$ is large. This leads to a nonzero energy gap for high disorder (see text).

D. Persistence of $E_{\rm gap}$ with disorder

To get a better understanding of the finite spectral gap $E_{\rm gap}$, it is useful to study the eigenfunctions for the low energy excitations. In Fig. 8 we show in gray-scale plots the local pairing amplitude $\Delta(\mathbf{r}_i)$ and $|u_n(\mathbf{r})|^2+|v_n(\mathbf{r})|^2$ for the lowest four excited state wave functions, for a particular realization of disorder at a high value of $V=3t$. We immediately notice the remarkable fact (which we have checked for many different realizations) that all the low-lying excitations live on the SC islands. Therefore it is no surprise that one ends up with a finite pairing gap.

The next question is: Why cannot one make a low-energy excitation that lives in the large ''sea,'' in between the SC islands, where there is no pairing gap? We argued earlier that the ''non-SC'' regions correspond, roughly speaking, to the high mountains and deep valleys in the random potential. It is not possible to inject an electron into a deep valley since it is already doubly occupied, and there is a large (potential) energy cost to extract an electron from such sites. Similarly, it is energetically unfavorable to create an electron on top of a high mountain in the random potential, and there are no electrons available to extract from such sites. Thus in the ''non-SC'' regions, the random potential does not permit low-energy excitations.

The lowest excitations then correspond to either injecting or extracting an electron from regions where $|V_i-\tilde{\mu}|$ is small, which are precisely regions with large $\Delta(\mathbf{r_i})$. Thus we see why these excitations have a finite pairing gap. (An understanding of the nonmonotonic behavior of $E_{\rm gap}$ and its eventual increase at large V will come from the analysis of Sec. IV.)

An immediate consequence of these ideas is that, while the islands may be thought of as locally superconducting, the sea separating them can be thought of as ''insulating'' with a large gap determined primarily by the random potential. This can be tested by the local density of states at different regions in the highly disordered regime as shown in Fig. 16.

E. Superfluid stiffness

It is important to understand how disorder, and in particular the formation of the inhomogeneous ground state, affects the phase rigidity. We calculate the superfluid stiffness D_s given by the usual Kubo formula[24]

$$\frac{D_s}{\pi}=\langle -k_x\rangle-\Lambda_{xx}(q_x=0,q_y\to 0,i\omega=0). \tag{8}$$

The first term $\langle -k_x\rangle$ is the kinetic energy along the x direction and represents the diamagnetic response to an external magnetic field. The second term is the paramagnetic response given by the (disorder-averaged) transverse current-current correlation:

$$\Lambda_{xx}(\mathbf{q},i\omega_n)=\frac{1}{N}\int_0^{1/T}d\tau\, e^{i\omega_n\tau}\langle j_x^p(\mathbf{q},\tau)j_x^p(-\mathbf{q},0)\rangle \tag{9}$$

with $j_x^p(\mathbf{q})$ the paramagnetic current and $\omega_n=2\pi nT$.

The stiffness calculated within the BdG approximation will be denoted by D_s^0 (D_s will be used for the renormalized stiffness defined later). Using Eq. (4) we find $\langle -k_x\rangle=(4t/N)\langle\Sigma_{\mathbf{r},n}v_n(\mathbf{r})v_n(\mathbf{r}+\hat{x})\rangle$, and at $T=0$

$$\begin{aligned}\Lambda_{xx}(1,2,i\omega_n=0)=2t^2\sum_{n_1,n_2}\frac{1}{(E+E')}[&v'(2+\hat{x})u(2)\\&+v(2+\hat{x})u'(2)]\times[u(1+\hat{x})v'(1)\\&+v(1)u'(1+\hat{x})-u(1)v'(1+\hat{x})\\&-v(1+\hat{x})u'(1)]+[u\leftrightarrow v,v\leftrightarrow u].\end{aligned} \tag{10}$$

Here $\hat{x}$ is the unit vector along x, and to simplify notation we use unprimed (primed) symbols to denote quantities with subscript $n1$ $(n2)$, and $r_i=1,r_j=2$. After disorder averaging we recover translational invariance, so that $\Lambda_{xx}(\mathbf{r}_i,\mathbf{r}_j,0)=\Lambda_{xx}(\mathbf{r}_i-\mathbf{r}_j,0)$ One can then Fourier transform to $\mathbf{q}$ to ob-

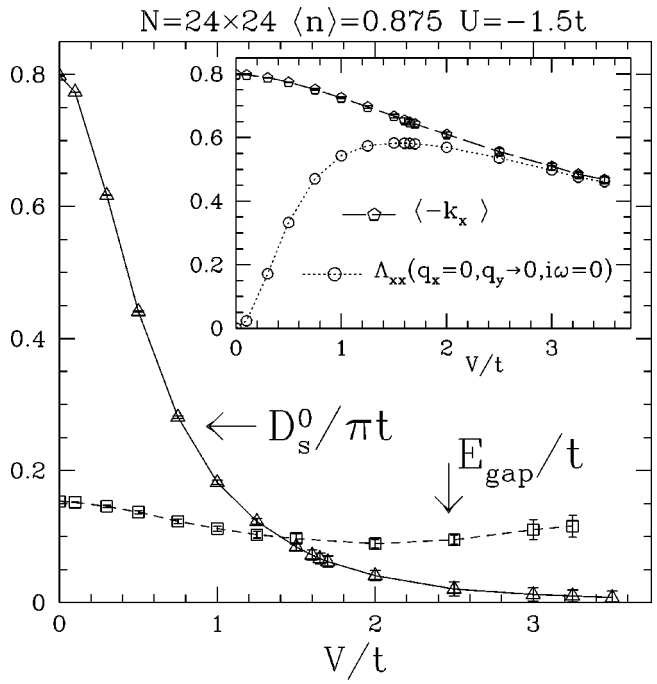

FIG. 9. The superfluid stiffness D_s^0/π calculated within the BdG theory as a function of disorder. The energy gap is also plotted for comparison. Note that, at $V=0$, $D_s^0 \gg E_{\rm gap}$, a characteristic of weak-coupling superconductors. However, at large disorder one finds $D_s^0 \ll E_{\rm gap}$ suggesting a phase fluctuation dominated regime. Inset: Disorder dependence of the diamagnetic and paramagnetic pieces of the response function (see text).

tain $\Lambda_{xx}(q_x=0,q_y,i\omega_n=0)$, which can be shown to vary as $A+Bq_y^2$ for small q_y. We verify this q_y dependence in our numerical results and use it to take the required limit in Eq. (8).

In Fig. 9 we show the behavior of the BdG phase stiffness D_s^0/π as a function of disorder. The very large reduction of D_s^0, by almost two orders of magnitude, can be intuitively understood by the following argument (which is also schematically illustrated in Fig. 10). Within mean-field theory the phases of the order parameter at different sites are completely aligned in the ground state. When an *external* phase twist θ is imposed the energy of the SC increases, leading to a nonzero superfluid stiffness $D_s^0 \sim d^2E(\theta)/d\theta^2$. In a uniform system the external twist is uniformly distributed throughout the system. However, in an disordered system where the amplitude is highly inhomogeneous the system will distribute the phase twists nonuniformly in order to minimize energy with most of the twist accommodated in regions where the amplitude is small. Thus an inhomogeneous system will be able to greatly reduce its superfluid stiffness D_s.[25]

We emphasize that despite this dramatic reduction in D_s^0, the superfluid stiffness continues to remain nonzero within the BdG approximation. In other words, the spatial variations in the pairing amplitude alone are unable to drive the system into an insulator. In order to describe the SIT it is therefore essential to take into account phase fluctuations as discussed in Sec. V below.

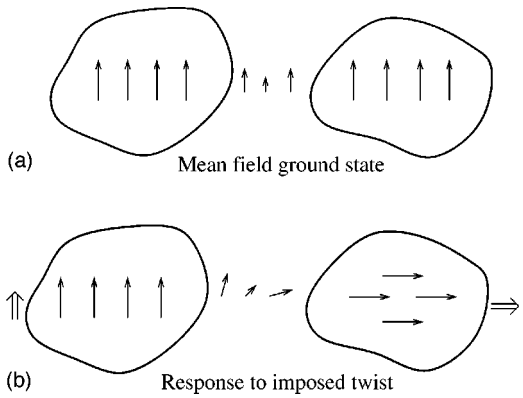

FIG. 10. (a) Schematic of a disordered SC in which the nonuniform amplitude results in the formation of SC islands. The length of the arrow denotes the amplitude and its direction the phase. Within mean-field theory the phase in the ground state is spatially uniform even though the amplitude is not. (b) Schematic illustration of the response to an externally applied phase twist (of $\pi/2$) indicated by the fat arrows. The system has a nonuniform response, with larger phase twists in regions where the amplitude is small. This results in a smaller stiffness $D_s^0 \sim d^2E(\theta)/d\theta^2$ compared to the case of a uniformly distributed phase twist.

F. Charge stiffness

The charge stiffness D^0 is the strength of $\delta(\omega)$ in the optical conductivity $\sigma(\omega)$ and is closely related to D_s^0. It is defined, after analytically continuing Λ_{xx} to real frequency[24]

$$D^0/\pi = \langle -k_x \rangle - \Lambda_{xx}(\mathbf{q}=\mathbf{0}, \omega \to 0). \tag{11}$$

Note the different order of limits compared with the definition of D_s. However, for a system with a spectral gap, on general grounds one expects that $D^0 = D_s^0$, as shown in Ref. 24. We have numerically checked this equality for all values of disorder. In fact, having established this, we chose to calculate D^0, rather than D_s^0, since on finite systems it is numerically easier to take the $\omega \to 0$ limit of $\Lambda_{xx}(0;\omega) \simeq A + B'\omega^2$, rather than calculate $\Lambda_{xx}(q_y \to 0)$.

IV. PAIRING OF EXACT EIGENSTATES

Although the BdG analysis described above led to various striking results and considerable physical insight, some issues could not be addressed. (1) We could not study the weak-coupling limit $|U|/t \ll 1$, since the exponentially large coherence length ξ leads to severe finite size effects in the numerical calculations. (2) Although the existence of the gap at large disorder could be understood, we did not get any insight into its nonmonotonic dependence on disorder.

In order to address these issues, and to gain a deeper understanding of the BdG results, we now generalize Anderson's original idea of pairing the time-reversed exact eigenstates of the disordered, *noninteracting* system,[3] in a manner that allows the local pairing amplitude to become spatially inhomogeneous. We will show that this generalization permits us to recover most, but not all, of the qualitative features of the BdG results. This analysis also has the virtue of leading to simpler equations from which one can gain qualitative

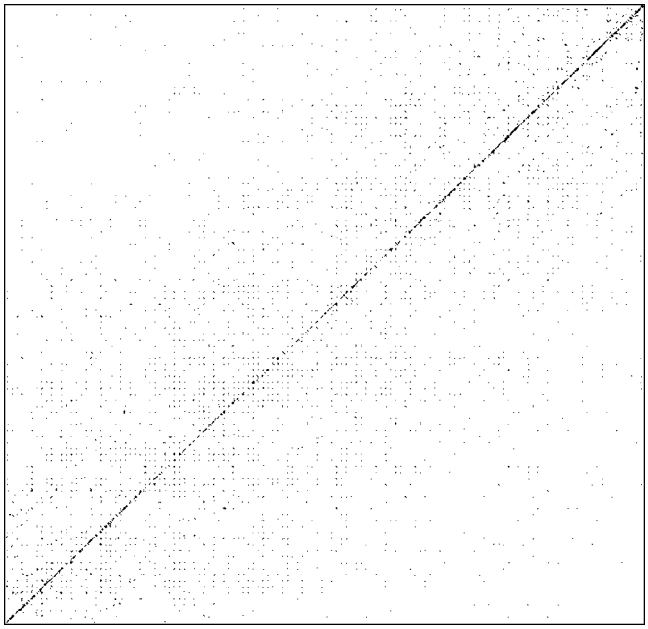

FIG. 11. Gray-scale plot of the matrix elements of $M_{\alpha,\beta}$ at large disorder $V=6t$ for a 30×30 noninteracting system. The x and y axes are the α and β indices, respectively. Note that diagonal matrix elements are the largest.

insights in the weak- and strong-disorder limits.

The noninteracting disordered Hamiltonian $\mathcal{H}_0$ of Eq. (1) is quadratic and leads to an eigenvalue problem, which is, in principle, soluble: $\mathcal{H}_0|\phi_\alpha\rangle=\varepsilon_\alpha|\phi_\alpha\rangle$, where α labels the exact eigenstates of $\mathcal{H}_0$. Following Anderson let us imagine pairing electrons in time-reversed eigenstates $\alpha,\uparrow$ and $\bar{\alpha},\downarrow$. The analog of the ''reduced BCS'' Hamiltonian in this basis is then given by

$$\mathcal{H}'=\sum_{\alpha,\sigma}\xi_\alpha c^\dagger_{\alpha\sigma}c_{\alpha\sigma}-|U|\sum_{\alpha,\beta}M_{\alpha,\beta}c^\dagger_{\alpha\uparrow}c^\dagger_{\bar{\alpha}\downarrow}c_{\bar{\beta}\downarrow}c_{\beta\uparrow}, \quad (12)$$

where the matrix $M_{\alpha,\beta}$ is defined by

$$M_{\alpha,\beta}=\sum_{\mathbf{r}_i}|\phi_\alpha(\mathbf{r}_i)|^2|\phi_\beta(\mathbf{r}_i)|^2. \quad (13)$$

Here $\xi_\alpha=(\varepsilon_\alpha-\tilde{\mu})$ is measured relative to the average Hartree-shifted $\tilde{\mu}$, which fixes the electronic density. (We will return to the question of average versus site-dependent Hartree shifts later in this section.) A BCS-like analysis of Eq. (12) leads to the $T=0$ gap equation

$$\Delta_\alpha=|U|\sum_\beta M_{\alpha,\beta}\frac{\Delta_\beta}{2E_\beta}, \quad (14)$$

where $E_\alpha=\sqrt{\xi_\alpha^2+\Delta_\alpha^2}$, and $\tilde{\mu}$ is determined by

$$\langle n\rangle=\frac{1}{N}\sum_\alpha\left(1-\frac{\xi_\alpha}{E_\alpha}\right). \quad (15)$$

Our formulation generalizes Anderson's original analysis by retaining the full $M_{\alpha,\beta}$, and it is the structure of this matrix that will permit us to access the large disorder regime with highly inhomogeneous pairing.

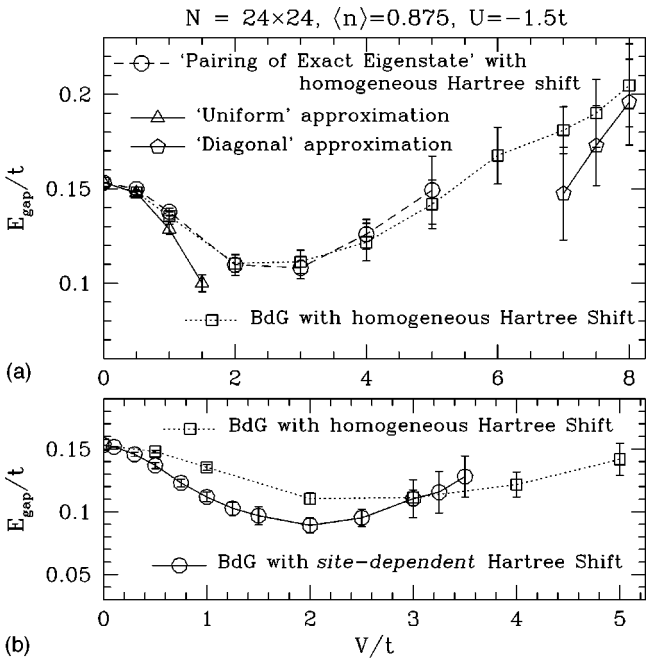

FIG. 12. Upper panel (a): Comparison of the energy gap $E_{\rm gap}$ as a function of disorder obtained by the generalized exact eigenstates method (○) and the BdG approach (□), both implemented with an average Hartree shift. Also shown are two asymptotic solutions for the gap at low (△) and high (pentagons) disorder. The decrease of $E_{\rm gap}$ at small V is a DOS effect, described by the ''uniform approximation'' (see text). The increase of $E_{\rm gap}$ at large V due to strong localization effects on the single-particle wave functions is described by the ''diagonal approximation'' (see text). Lower panel (b): Comparison of $E_{\rm gap}$ as a function of disorder calculated within the BdG approach with an average and a site-dependent Hartree shift. While the two results are qualitatively similar, there are quantitative differences.

A. Nonmonotonic behavior of the energy gap

We now present a qualitative analysis of the large and small disorder limits of the above equations, together with their full numerical solution. Finally, these will be compared with the BdG results of the previous section.

Let us begin with the low disorder regime. For a finite system in two dimensions, or an infinite system in three dimensions, the eigenstates $\phi_\alpha(\mathbf{r}_i)$'s are extended on the scale of system. We thus find $M_{\alpha,\beta}\approx1/N$, independent of α and β, which we call the ''uniform approximation'' for M. The gap equation takes the simple BCS form, Δ is (spatially) uniform, and Anderson's theorem applies in this limit.

The behavior of $E_{\rm gap}$ within ''uniform approximation'' is shown in Fig. 12(a) for low V. The decrease of $E_{\rm gap}$ with increasing V in this regime can be traced primarily to a simple density-of-states effect in the BCS result for the gap. For the nearest-neighbor 2D dispersion and the filling chosen, one finds that the average DOS at the chemical potential, $\bar{N}(\xi=0)$, decreases with increasing V in the weak-disorder limit.

In the high-disorder regime, on the other hand, the eigenstates of the noninteracting problem are strongly localized and different states have a very small spatial overlap. We can therefore make a ''diagonal approximation'' for for the M matrix: $M_{\alpha,\beta} \approx \delta_{\alpha,\beta} \Sigma_{\mathbf{r}_i} |\phi_\alpha(\mathbf{r}_i)|^4$. We have numerically checked that the diagonal elements of M are indeed the largest elements as shown in Fig. 11. Moreover, the off-diagonal elements are not important in the gap equation (14), as states that are nearby in space are far in energy and vice versa. Next we identify $\Sigma_{\mathbf{r}_i} |\phi_\alpha(\mathbf{r}_i)|^4$ as the participation ratio for the (normalized) state $\phi_\alpha(\mathbf{r}_i)$, which in turn is given by $\zeta_{\rm loc}^{-2}(\alpha)$, where $\zeta_{\rm loc}(\alpha)$ is the localization length for that state.[18]

Thus for large disorder we solve the gap equation (14) with the kernel $M_{\alpha,\beta} \approx \delta_{\alpha,\beta} \zeta_{\rm loc}^{-2}(\alpha)$. We find that for states α with energies far from the chemical potential, the solution is $\Delta_\alpha = 0$, i.e., these states are unaffected by pairing. On the other hand, for states with small ξ_α we find $E_\alpha \simeq |U|/[2\zeta_{\rm loc}^2(\alpha)]$. One thus obtains a gap

$$E_{\rm gap} = \frac{|U|/2}{\zeta_{\rm loc}^2} \tag{16}$$

in the high-disorder limit, where $\zeta_{\rm loc}$ is the localization length of the state at the chemical potential.

The diagonal approximation becomes exact in the extreme site localized limit ($V \to \infty$). In this case, the exact eigenstate label α is the site $\mathbf{r}_i$ at which the state is localized. It is easy to show that all states for which $\xi_{r_i} < |U|/2$ have finite pairing amplitude and a spectral gap of $|U|/2$, which is a well-known result.[9] (For another approach to the large-disorder limit, see Ref. 26.)

In Fig. 12(a) we compare the small- and large-disorder asymptotic results, i.e., the ''uniform'' and ''diagonal'' approximations, with the spectral gap obtained from a full numerical solution of Eqs. (14) and (15) of the method of exact eigenstates (where we self-consistently determined Δ_α's for *all* α's and $\tilde{\mu}$). Finally we also show in Fig. 12(a) the BdG solution for $E_{\rm gap}$, with a *uniform* Hartree shift, which is in excellent agreement with the exact eigenstates result. [Similar agreement is also found for all the other quantities such as $P(\Delta), \Delta_{\rm OP}, N(\omega)$, and D_s^0 as a function of V.]

To summarize: we now have a complete understanding of the nonmonotonic dependence of the spectral gap on disorder. The weak disorder asymptote shows that the initial drop is a simple density-of-states effect. On the other hand, the increase of the gap in the strong-disorder limit comes from the decrease in the localization length $\zeta_{\rm loc}$ as seen from Eq. (16).

It is important to emphasize that while the numerical comparisons in Fig. 12(a) are for a moderate value of $|U| = 1.5t$, the method of pairing of exact eigenstates should work best in the weak-coupling limit, where $|U|$ is the smallest energy scale in the problem, and hence the noninteracting problem is diagonalized first. The analytical approximations in the small- and large-disorder limits given above are thus valid even for $|U|/t \ll 1$ where we cannot do reliable numerical calculations.

B. SC islands and low-lying excitations

The exact eigenstates formulation also gives analytical insight into the large spatial overlap of the low-lying excited states with the SC islands in the large disorder regime, which was observed and discussed at length in the previous section. One can show quite generally that the pairing amplitude in real space $\Delta(\mathbf{r})$ is related to Δ_α through $\Delta_\alpha = \Sigma_{\mathbf{r}_i} \Delta(\mathbf{r}_i) |\phi_\alpha(\mathbf{r}_i)|^2$. The gap equation (14) can then be rewritten as

$$\Delta(\mathbf{r}_i) = \frac{|U|}{2} \sum_\alpha \frac{\Delta_\alpha}{\sqrt{\xi_\alpha^2 + \Delta_\alpha^2}} |\phi_\alpha(\mathbf{r}_i)|^2. \tag{17}$$

We now specialize to the large-disorder regime and use the solution of the gap equation within the ''diagonal approximation'' in the preceding subsection to note that the only α's that contribute to the sum are those with $\xi_0 \approx 0$, since otherwise $\Delta_\alpha = 0$. The above equation then simplifies to $\Delta(\mathbf{r}_i) \approx |U| \Sigma'_\alpha |\phi_\alpha(\mathbf{r}_i)|^2/2$ with the sum restricted to states near the chemical potential. This immediately shows the strong correlation between the spatial structures of the regions of $\Delta(\mathbf{r}_i)$, the SC islands, and that of the eigenstates $\phi_\alpha(\mathbf{r}_i)$ of the noninteracting problem, which are the low-lying excitations.

C. Importance of site-dependent Hartree shifts

Having seen the great success of the exact eigenstates method in reproducing the BdG results, we finally turn to the one important feature of the BdG analysis that is *not* captured by this method. We saw in Eq. (3) that the BdG equations incorporate site-dependent Hartree shifts, while the method of exact eigenstates did not. We now discuss the effects of inhomogeneous Hartree terms and why such terms are not easy to deal with in the exact eigenstates formalism. We are not aware of any previous work that has looked at the effects of such inhomogeneous Hartree shifts.

First, inclusion of site-dependent Hartree terms leads to quantitative differences with the uniform (average) Hartree approximation for $E_{\rm gap}$ as a function of V as seen from the lower panel of Fig. 12.

Second, a much more dramatic qualitative effect can be seen in the DOS plotted in Fig. 13. The calculation with an average Hartree shift has a BCS-like pile-up in the DOS at the gap edge, while the result with the site-dependent shifts shows that this pile-up is completely smeared out with states pushed out to the band tails. The occurrence of the DOS peak within the theory of exact eigenstates (with homogeneous Hartree shift) has the same origin as that in BCS theory. The inhomogeneity in the Hartree shift acts like a random perturbation that breaks the degeneracy of states near the gap edge.

It would have been nice to incorporate a site-dependent Hartree shift in the exact eigenstates approach. However, in this case the ''normal state'' Hamiltonian whose exact eigenstates one would have to solve for would be

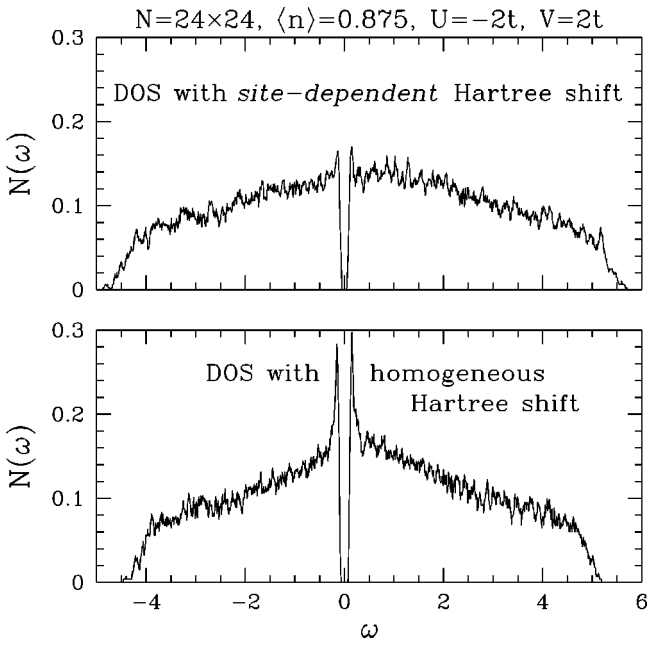

FIG. 13. Comparison of the density of states obtained from the BdG analysis that includes the local self-consistent Hartree shift (top panel) with the result of the exact eigenstates method with an average Hartree shift (bottom panel). The latter leads to a spurious pile-up in the DOS at the gap edge.

$$\mathcal{H}_{\text{normal}} = -t \sum_{\langle ij \rangle, \sigma} (c^{\dagger}_{i\sigma} c_{j\sigma} + \text{H.c.}) + \sum_{i,\sigma} (V_i - \mu - |U| \langle n_i \rangle / 2) n_{i\sigma}.$$

One then loses much of the simplicity of the exact eigenstate formalism since $\mathcal{H}_{\text{normal}}$ is itself an *interacting* problem, which needs to be solved self-consistently. Further, there are problems (which we will not discuss here) associated with treating U at the Hartree level alone, before incorporating pairing, in the large-disorder regime.[27]

In conclusion, while the generalized pairing of exact eigenstates is able to give much insight into the behavior of the spectral gap and pairing amplitudes, and gives qualitative information about the weak-coupling limit, the BdG method with site-dependent Hartree shifts is the best scheme for quantitative results.

V. QUANTUM PHASE FLUCTUATIONS

In Sec. III E, we found that the BdG analysis leads to a large suppression of the superfluid stiffness, but the disorder-induced amplitude inhomogeneity is not sufficient to drive D_s to zero. In order to understand the transition to an insulating state, we must focus on the phase degrees of freedom which are ignored (or frozen) in the mean-field description used thus far. We use the 2D quantum XY action in imaginary time to describe the dynamics of the phase variables $\theta(\mathbf{r}, \tau)$ defined on a coarse-grained square lattice of lattice spacing ξ:

$$S_{\theta} = \frac{\kappa \xi^2}{8} \int_0^{\beta} d\tau \sum_{\mathbf{r}} \left(\frac{\partial \theta(\mathbf{r}, \tau)}{\partial \tau} \right)^2 + \frac{D_s^0}{4} \int_0^{\beta} d\tau \times \sum_{\mathbf{r}, \boldsymbol{\delta}} \{1 - \cos[\theta(\mathbf{r}, \tau) - \theta(\mathbf{r} + \boldsymbol{\delta}, \tau)]\}. \quad (18)$$

We can motivate the use of an XY model in both the weak- and strong-disorder limits, and therefore use it for all disorder strengths. At weak disorder, one can follow the derivation of Ref. 11 to derive an effective action for the phase variables in a disordered system, and then coarse grain to the scale of ξ using the method of Ref. 28 to obtain the above action. This coarse graining shows that the coefficient of the time derivative term is $\xi^2 \kappa$ in two dimensions where $\kappa = dn/d\mu$ is the static, long-wavelength compressibility calculated at the mean-field level, and the coefficient of the cosine term is the mean-field phase stiffness D_s^0.

In the opposite high-disorder limit one can view Eq. (18) as describing a Josephson junction array of the SC islands embedded in an insulating sea (see Fig. 6). In this case, the first term represents the charging energy of the islands and the second term the Josephson coupling between islands. Further we make the crude approximation of ignoring the random variations of the charging and coupling energies in this random system, and simply using the mean-field values obtained from the BdG analysis. We also ignore the disorder dependence of the coherence length ξ, and for simplicity use its $V = 0$ value ξ_0.

The nonlinearities in the cosine term lead to a renormalization of the stiffness. Within the self-consistent harmonic approximation[29] (SCHA), this is determined by choosing the optimal Gaussian action

$$S_0 = \frac{\kappa \xi^2}{8} \int_0^{\beta} d\tau \sum_{\mathbf{r}} \left(\frac{\partial \theta(\mathbf{r}, \tau)}{\partial \tau} \right)^2 + \frac{D_s}{8} \int_0^{\beta} d\tau \sum_{\mathbf{r}, \delta} [\theta(\mathbf{r}, \tau) - \theta(\mathbf{r} + \boldsymbol{\delta}, \tau)]^2, \quad (19)$$

which minimizes the free energy. The renormalized stiffness D_s is given by[29]

$$D_s = D_s^0 \exp(-\langle \theta_{ij}^2 \rangle_0 / 2). \quad (20)$$

Here $\langle \theta_{ij}^2 \rangle_0$ is the mean square fluctuation of the near-neighbor phase difference

$$\langle \theta_{ij}^2 \rangle_0 = \frac{2}{N\xi} \sum_{\mathbf{Q}} \left[\frac{\varepsilon_{\mathbf{Q}}}{D_s \kappa} \right]^{1/2}, \quad (21)$$

with $\varepsilon_{\mathbf{Q}} = 2[2 - \cos(Q_x) - \cos(Q_y)]$, and the momentum sum is restricted to $Q_i < \pi$.

Defining the renormalization factor $X = D_s / D_s^0$, and

$$\sqrt{\alpha} = \frac{1}{\xi \sqrt{D_s^0 \kappa}} \left(\frac{1}{N} \sum_{\mathbf{Q}} \varepsilon_{\mathbf{Q}}^{1/2} \right), \quad (22)$$

one can write Eq. (20) as

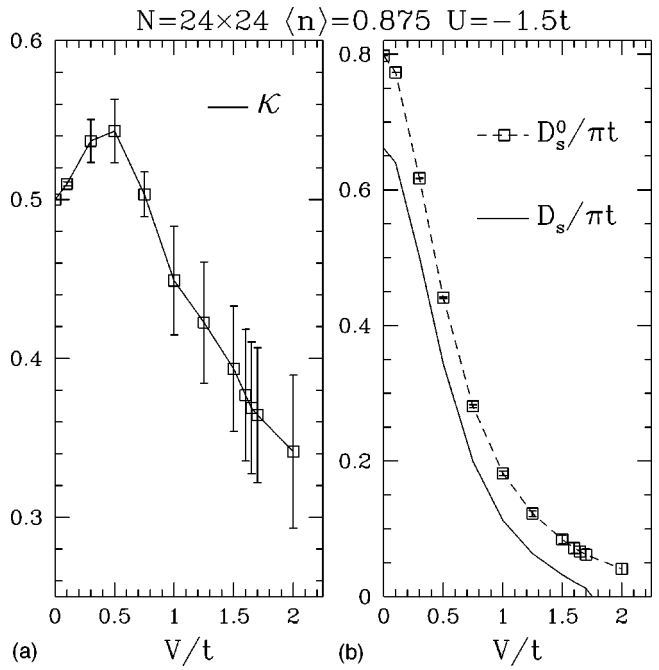

FIG. 14. (a) Left panel: The compressibility $\kappa = dn/d\mu$ as a function of disorder V. (b) Right panel: Evolution of superfluid stiffness D_s/π upon including the quantum phase fluctuations. The bare BdG stiffness D_s^0 is plotted as symbols with a dashed line through them, while the renormalized stiffness D_s/π is shown by the full line. D_s vanishes at $V_c = 1.75t$ beyond which the system is insulating.

$$X = \exp(-\sqrt{\alpha/X}). \tag{23}$$

We solve Eq. (23) to determine the renormalized $D_s(V)$, using as input for α the BdG results for the bare stiffness D_s^0 and compressibility κ for each value of V. The BdG compressibility is plotted in Fig. 14(a). We do not have a simple physical picture for the small maximum in κ at low disorder, which is a parameter-dependent feature absent for larger values of $|U|$. However, our results for the renormalization of D_s are insensitive to the presence or absence of this nonmonotonicity.

The renormalized D_s obtained from the SCHA is plotted in Fig. 14(b) as the full line. Quantum phase fluctuations lower the stiffness and beyond a certain critical disorder drive it to zero, unlike the bare (BdG) stiffness, which is always nonzero. Thus the SCHA gives a transition to a nonsuperconducting state, even though it is unreliable in the vicinity of the transition. In particular, Eq. (23) predicts a transition at $\alpha_{\rm crit} = 4\exp(-2)$ with a jump discontinuity of $\exp(-2)$ in the value of X. We believe that this discontinuity is an artifact of the approximation, although the critical disorder obtained from such a calculation is in reasonable agreement with quantum Monte Carlo results[17] for parameter values ($|U|/t = 4$) for which a comparison can be made.[14]

We next argue that quantum phase fluctuations do *not* have a significant effect on the electronic excitation spectrum. This is because the spectral gap at large disorder arises from low-energy excitations that live *on* a SC island, which is relatively unaffected by phase fluctuations. On the other hand, as we have seen above, these fluctuations have a profound effect on suppressing the coherence *between* SC islands. Thus the nonsuperconducting state continues to have a finite spectral gap for one-electron excitations even after the effects of phase fluctuations are included, and is an insulator. Finally the absence of low-lying electronic excitations near the transition implies that the quantum phase transition in this electronic model is in the superfluid-Bose insulator universality class.[15]

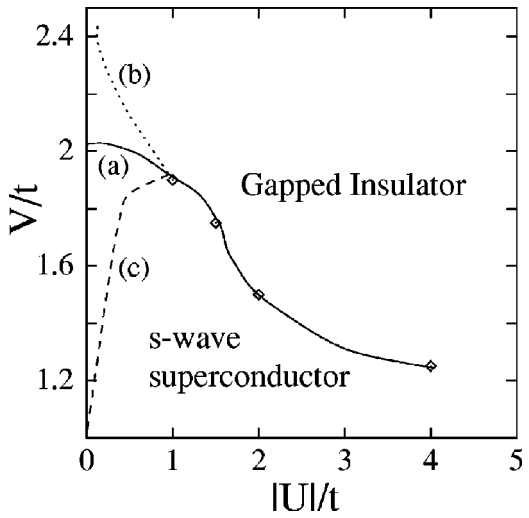

FIG. 15. Schematic phase diagram at $T = 0$ of the disordered, attractive Hubbard model in the disorder-attraction (V-$|U|$) plane. The entire y axis ($|U|/t = 0$) corresponds to an Anderson insulator with gapless excitations. At finite $|U|/t$ there are two phases: a SC phase at low disorder and a gapped insulating phase at high disorder. Thus U is a singular perturbation in that the smallest $|U|$ induces a gap. The symbols denote the critical disorder $V_c(U)$, separating the SC and the insulating phases, estimated from the calculations described in the text. We argue against possibilities (b) and (c) for the form of the phase boundary in the $|U| \to 0$ limit, and suggest that $V_c(U \to 0)$ approaches a finite value of order unity, as shown schematically by curve (a). We find no evidence for a gapless Fermi insulator phase at nonzero $|U|/t$.

VI. PHASE DIAGRAM

In this section we discuss the $T = 0$ phase diagram for the disordered, attractive Hubbard model in the $(|U|/t, V/t)$ plane. It is known[18] that, on the $|U| = 0$ axis, for all values of disorder $V \neq 0$, one has an Anderson insulator with gapless excitations in two dimensions. On the $V = 0$ axis one simply has a crossover as a function of $|U|/t$ from a BCS superconductor to a condensate of interacting (hard core) bosons.[30]

The four symbols marked in Fig. 15 are the result of a BdG analysis supplemented by the simple phase fluctuation analysis described above. Despite the simplifying approximations involved, and the lack of a detailed study of finite size effects, we nevertheless believe that our results do give a reasonable qualitative idea about the critical disorder $V_c(U)$ separating the SC phase from an insulator with a gap in its single-particle excitation spectrum. Further, our estimated V_c at $|U|/t = 4$ is in reasonable agreement[14] with quantum Monte Carlo results.[17]

In principle, there are three possibilities for the continuation of the $V_c(U)$ phase boundary as $|U|/t \to 0$, a limit which we cannot address numerically. As shown in Fig. 15 these are (a) $V_c(U \to 0)$ is a finite number of order unity; (b) $V_c(U \to 0)$ diverges to infinity; or (c) $V_c(U \to 0)$ vanishes. We will now argue against (b) and (c), suggesting that (a) is in fact the correct result.

First we examine possibility (b) by looking at the case of a fixed small $|U|/t$ with $V \to \infty$. From the large-disorder asymptotics of the preceding section (within the ''diagonal approximation'' for the matrix M) we found that one obtains SC islands whose size is the localization length. Thus the effective coherence length is determined by $\zeta_{\rm loc}$, i.e., the disorder and not by the weak coupling. Since this length scale becomes very small for large V, we expect phase fluctuations to destroy the long-range phase coherence between the small SC islands. Thus we find it very hard for SC to persist out to very large disorder as required by possibility (b).

Next consider possibility (c) by studying the case of a fixed, small V taking the limit $|U|/t \ll 1$. Here one can just use the standard theory of dirty superconductors. The pure $(V=0)$ coherence length ξ_0 is exponentially large in $|U|/t$, and even if the coherence length in the disordered problem is given by $\xi \sim \sqrt{\xi_0 l}$, ξ nevertheless grows as $|U|/t$ is reduced. With a growing coherence length, both amplitude and phase fluctuations are suppressed, and we cannot see how SC can be destroyed as required by possibility (c).

There have been suggestions[31] from QMC studies of *two* insulating phases: a gapless ''Fermi'' insulator at small $|U|$ and a gapped ''Bose'' insulator at large $|U|$ for the model in Eq. (1). It is possible that a vanishing gap may have been observed because of the finite temperature in the simulations. We see absolutely no evidence for a ''Fermi'' insulator, away from the $|U|=0$ line, and we have presented strong numerical evidence and arguments for a finite gap in the non-SC state for any $|U|>0$.

In the $|U|/t \gg 1$ our Hamiltonian maps on to the problem of hard core interacting bosons, with an effective hopping $t_{\rm Bose} \sim t^2/|U|$, in a random potential. For this problem one expects $V_c(|U| \to \infty) \sim t^2/|U|$, which gives us an understanding of the decrease in V_c with $|U|$. Further, in this limit the insulating phase is precisely the Bose glass phase.[15]

VII. EXPERIMENTAL IMPLICATIONS

In this section we discuss some implications of our results for experiments.[32]

A. Prediction for STM measurement

In Sec. III C we showed that, at large disorder, the system consists of ''SC islands'' with significant pairing amplitude that are separated from each other by an insulating sea. We also discussed in detail that the spectral gap in the insulating regions (determined mainly by the random potential) is larger than the pairing gap on the SC islands. This is most clearly seen in our results for the local density of states (LDOS) plotted in Fig. 16. Further, the SC regions (upper panel) show, as expected, a large pile-up in the DOS at the gap edge, while the non-SC regions (lower panel) have no such pile-up and instead the states are spread out over a large energy range, features often associated with pseudogaps in other contexts. It should be possible to measure the LDOS using an STM probe, as has already been demonstrated in other systems [magnetic impurities in *s*-wave SC (Ref. 33) and impurities in the high-T_c *d*-wave SC (Refs. 34 and 35)].

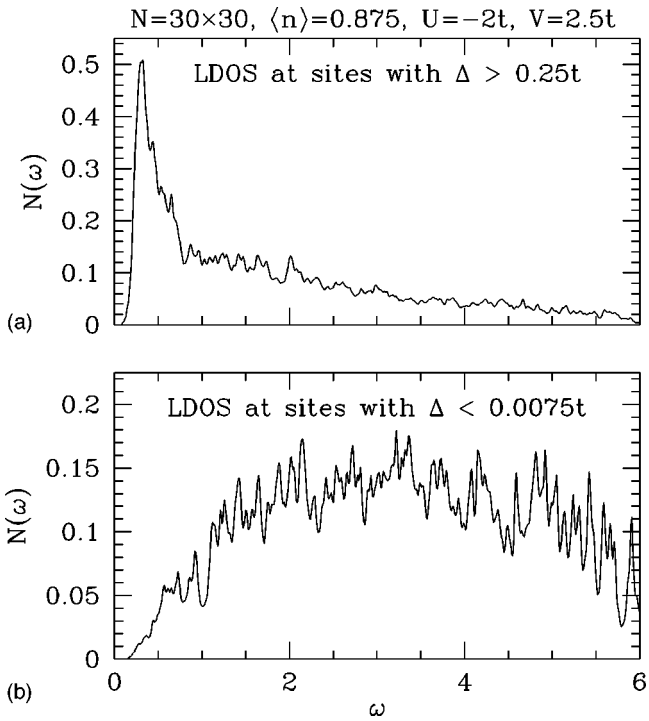

FIG. 16. (a) Upper panel: The local density of states (LDOS) at sites where the pairing amplitude Δ is large. These regions correspond to the ''SC islands'' which have a small local superconducting gap and a coherence peak at the gap edge. (b) Lower panel: LDOS at sites with $\Delta \approx 0$. These regions correspond to the ''insulating sea'' showing a larger spectral gap, without any coherence peak features at the gap edge, reminiscent of pseudogap behavior.

B. "Homogeneously" disordered versus granular systems

Depending on the material, the substrate, and growth conditions it is experimentally possible to grow two types of films: (a) ''homogeneously'' disordered films[36] that are disordered on an atomic scale and (b) granular films.[37,38] It is often argued that the nature of the SC-insulator transition (SIT) in these two types of films is quite distinct. The SIT in ''homogeneous'' films is thought to be driven by the collapse of the SC amplitude as a function of disorder, whereas that in the granular film category (b) is driven by the loss of phase coherence.

Our work shows that this distinction is not valid, at least for the model studied. Even though our model is ''homogeneously'' disordered on a microscopic scale, with increasing disorder the system self-organizes into a nanoscale granular structure in terms of the local pairing amplitude. In the high-disorder regime, the inhomogeneous state consists of SC is-

lands whose phases are Josephson coupled through the insulating regions between the islands. As described in detail in Sec. V it is the competition between the charging energy of the islands and the Josephson coupling that leads to the SIT at $T=0$. In the highly disordered regime we expect that, as temperature is reduced, SC sets in in two steps: first the individual SC islands become superconducting but they are not phase coherent, and the system is in a resistive state. As the temperature is lowered the Josephson coupling between the SC islands leads to global phase coherence at T_c.

ACKNOWLEDGMENTS

We would like to thank Allen Goldman, Art Hebard, Arun Paramekanti, Subir Sachdev, and Jim Valles for useful discussions. M.R. was supported in part by the DST under the Swarnajayanti scheme.

[1] A. Hebard, in *Strongly Correlated Electronic Systems*, edited by K. Bedell *et al*. (Addison-Wesley, New York, 1994).

[2] A. M. Goldman and N. Marković, Phys. Today **51** (11), 39 (1998).

[3] P. W. Anderson, J. Phys. Chem. Solids **11**, 26 (1959).

[4] A. A. Abrikosov and L. P. Gorkov, Zh. Éksp. Teor. Fiz. **36**, 319 (1959) [Sov. Phys. JETP **9**, 220 (1959)].

[5] D. Belitz and T. Kirkpatrick, Rev. Mod. Phys. **66**, 261 (1994).

[6] M. Sadovskii, Phys. Rep. **282**, 225 (1997).

[7] A. I. Larkin and Y. N. Ovchinnikov, Zh. Éksp. Teor. Fiz. **61**, 2147 (1971) [Sov. Phys. JETP **34**, 1144 (1972)].

[8] H. Fukuyama, H. Ebisawa, and S. Maekawa, J. Phys. Soc. Jpn. **53**, 3560 (1984).

[9] M. Ma and P. A. Lee, Phys. Rev. B **32**, 5658 (1985).

[10] G. Kotliar and A. Kapitulnik, Phys. Rev. B **33**, 3146 (1986).

[11] T. V. Ramakrishnan, Phys. Scr. **T27**, 24 (1989).

[12] R. A. Smith and V. Ambegaokar, Phys. Rev. B **45**, 2463 (1992).

[13] A. M. Finkel'stein, Physica B **197**, 636 (1994).

[14] A. Ghosal, M. Randeria, and N. Trivedi, Phys. Rev. Lett. **81**, 3940 (1998).

[15] M. P. A. Fisher, G. Grinstein, and S. M. Girvin, Phys. Rev. Lett. **64**, 587 (1990).

[16] The importance of spatial amplitude fluctuations in the dirty boson problem was emphasized by K. Sheshadri, H. R. Krishnamurthy, R. Pandit, and T. V. Ramakrishnan, Phys. Rev. Lett. **75**, 4075 (1995).

[17] N. Trivedi, R. T. Scalettar, and M. Randeria, Phys. Rev. B **54**, R3756 (1996); R. T. Scalettar, N. Trivedi, and C. Huscroft, *ibid.* **59**, 4364 (1999).

[18] P. A. Lee and T. V. Ramakrishnan, Rev. Mod. Phys. **57**, 287 (1985).

[19] The effect of disorder on the Coulomb interactions through μ^* has been studied (see Ref. 5 and references therein). However, Coulomb interactions in an inhomogeneous system could produce qualitatively new effects. For example, (a) the effective attraction between electrons could become inhomogeneous producing regions where the pairing amplitude is suppressed with locally gapless excitations. (b) Coulomb effects plus disorder could produce local moments that could be pair breaking. [M. Milovanovic, S. Sachdev, and R. N. Bhatt, Phys. Rev. Lett. **63**, 82 (1989); S. Sachdev, Philos. Trans. R. Soc. London, Ser. A **356**, 173 (1998)]. These are important directions for further study.

[20] For $|U|=1.5t$ and $\langle n\rangle=0.875$, we estimate, from the asymptotic decay of the BCS pair wave function, that the pure ($V=0$) limit coherence length $\xi_0\simeq 10$ (in units of the lattice spacing). In the presence of disorder, the coherence length can only be smaller than this estimate.

[21] P. G. de Gennes, *Superconductivity in Metals and Alloys* (Benjamin, New York, 1966).

[22] T. Xiang and J. M. Wheatley, Phys. Rev. B **51**, 11 721 (1995); M. Franz, C. Kallin, A. J. Berlinsky, and M. I. Salkola, *ibid.* **56**, 7882 (1997); W. A. Atkinson, P. J. Hirschfeld, and A. H. Macdonald, Phys. Rev. Lett. **85**, 3922 (2000).

[23] A. Ghosal, M. Randeria, and N. Trivedi, Phys. Rev. B **63**, 020505(R) (2000).

[24] D. J. Scalapino, S. R. White, and S. C. Zhang, Phys. Rev. B **47**, 7995 (1993).

[25] This idea can be used to obtain an upper bound on D_s as shown by A. Paramekanti, N. Trivedi, and M. Randeria, Phys. Rev. B **57**, 11 639 (1998).

[26] I. Herbut, Int. J. Mod. Phys. B **14**, 575 (2000).

[27] A. Ghosal, Ph.D. thesis, Tata Institute of Fundamental Research, 2000.

[28] A. Paramekanti, M. Randeria, T. V. Ramakrishnan, and S. S. Mandal, Phys. Rev. B **62**, 6786 (2000).

[29] D. Wood and D. Stroud, Phys. Rev. B **25**, 1600 (1982); S. Chakravarty, G.-L. Ingold, S. Kivelson, and A. Luther, Phys. Rev. Lett. **56**, 2303 (1986).

[30] For a review, see M. Randeria, in *Bose-Einstein Condensation*, edited by A. Griffin, D. Snoke, and S. Stringari (Cambridge University Press, Cambridge, 1995).

[31] C. Huscroft and R. T. Scalettar, Phys. Rev. Lett. **81**, 2775 (1998).

[32] One must keep in mind here that the main assumption of our model is the neglect of Coulomb interactions as discussed in Sec. II and Ref. 19.

[33] A. Yazdani, B. A. Jones, C. P. Lutz, M. F. Crommie, and D. M. Eigler, Science **275**, 1767 (1997).

[34] T. Cren, D. Roditchev, W. Sacks, J. Klein, J. B. Moussy, C. Deville-Cavellin, and M. Lagues, Phys. Rev. Lett. **84**, 147 (2000).

[35] S. H. Pan *et al.* (unpublished).

[36] D. B. Haviland, Y. Liu, and A. M. Goldman, Phys. Rev. Lett. **62**, 2180 (1989); J. M. Valles, R. C. Dynes, and J. P. Garno, *ibid.* **69**, 3567 (1992).

[37] A. E. White, R. C. Dynes, and J. P. Garno, Phys. Rev. Lett. **33**, 3549 (1986); H. M. Jaeger, D. B. Haviland, A. M. Goldman, and B. G. Orr, Phys. Rev. B **34**, 4920 (1986).

[38] D. Shahar and Z. Ovadyahu, Phys. Rev. B **46**, 10 917 (1992).